Nonlinear response of electric fields at a neutral point

Mikhail Berkovsky and James W. Dufty
Department of Physics, University of Florida, Gainesville, Florida 32611

Annette Calisti, Roland Stamm, and Bernard Talin
Equipe Diagnostics dans le Gaz et les Plasmas, URA 773, Université de Provence, Centre de St. Jérome 13397 Marseille Cedex 13, France

(Received 28 December 1994)

The complex dynamics of electric fields at a neutral point in a plasma is studied via a model of noninteracting "quasiparticles." The simplicity of the model allows the reduction of the many-body problem to an effective single-particle analysis — all properties of interest can be reduced to quadratures. Still, the final calculations to extract a quantitative or even qualitative understanding of the field dynamics can be difficult. Attention here is focused on the dynamics of the conditional electric field: the field value at time t for a given initial value of the field. In addition to the relevant linear response function (electric field time correlation function), this property provides the complete nonlinear response of the electric field to arbitrary initial field perturbations. The static properties (distribution of electric fields and field time derivatives) and the electric field time correlation function have been known for some time for this model. We compare these results and the present result for the conditional electric field with molecular dynamics simulations *including* interactions. The comparisons suggest that the model provides a quantitative representation of electric field dynamics in real plasmas, except at strong coupling. The exact theoretical results are compared also with those obtained by modeling the electric field as a stochastic variable obeying a kangaroo process. The latter can be constructed to yield both the exact stationary distribution and the exact electric field time correlation function. However, we find that the conditional field is never well approximated by this process. An alternative representation of the joint distribution for electric fields, consistent with the exact stationary distribution, field correlation function, and conditional electric field, is suggested.

PACS number(s): 51.70.+f, 51.90.+r

I. INTRODUCTION

The structural and dynamical properties of a plasma can be studied using a test charge to measure the total electric field at an arbitrary point. Two cases are of interest: (i) the field at a finite test charge and (ii) the field at a vanishingly small test charge. In the former case, the test charge influences the plasma charge configuration near it in an important way; in the second case, the test charge has negligible effect and acts as a passive probe of the plasma. In the following, attention will be limited to this second case, the electric field at a "neutral" point. A related analysis of the charged point case will be discussed elsewhere.

There is an intrinsic value to the detailed study of electric field distributions and dynamics as a representation of the complex collective dynamics in charged systems. For example, the electric field autocorrelation function provides a rich description of the linear response of the plasma to a single external charge. The objective here is to explore the more general nonlinear response characteristics associated with higher-order correlation functions. There are also very practical reasons to have an understanding of the nonlinear electric field response at a neutral point. The spectral lines emitted by neutral atoms or molecules in a plasma are sensitive to their environment and couple to it primarily via a dipole interaction. The electric field history over the radiation times, for each possible initial value in the ensemble considered, provides the only relevant property of the surrounding plasma. Indeed, the most successful method for calculating line shapes at present is based on solution to the Schrödinger equation for dipole radiation, using an electric field history determined from molecular dynamics simulation [1]. A theoretical alternative, also successful, replaces the molecular dynamics simulation by a presumed stochastic process to determine the electric field dynamics [2]. Our objective is a theoretical study of electric field dynamics at the more fundamental level of statistical mechanics. Determination of the electric field requires knowledge of the trajectories of all plasma particles and consequently a detailed confrontation of the many-body problem. Progress can be made at this fundamental level either by restricting attention to simple properties (e.g., field correlations) or by idealizing the plasma to allow the study of more complex properties. Here we choose the latter approach and consider an ideal gas of charges that generate electric fields, but are unaffected by the fields of other particles. The trajectories are then straight lines and all dynamical aspects of the many-body problem are obviated. The collective ef-

fects obtained therefore are associated with the statistical properties of the ensemble of initial states considered.

Historically, this idealized model has provided important insight for understanding the static properties of fields. It was used by Holtsmark [3] 75 years ago for the probability distribution of electric field values in plasmas and by Chandresekhar [4] 35 years ago for the distribution of gravitational fields in astrophysical structures. Surprisingly, there have been few studies of field dynamics for this model [5,6]. The fields due to these independent particles can be chosen as Coulomb fields, to represent rapidly moving electrons, or screened Coulomb fields for more slowly moving ions. In the Coulomb case, the predictions of this model are only qualitative, but for screened Coulomb interactions they provide a quantitative description as well (except at strong coupling). We verify this claim for several static and dynamic properties by comparing with results from molecular dynamics simulations that include interactions among particles. Thus, for screened fields both the qualitative and the quantitative features of electric fields determined here can be considered as representative of those in real plasmas.

As might be expected, the absence of interactions among particles allows the reduction of any property of interest to quadratures. This is demonstrated in Appendix A, where the generating functional for multitime electric field correlation functions of arbitrary degree is calculated. This generating functional also determines the relative probability for *any* chosen function $\vec{\mathcal{E}}(t)$ to represent the electric field history over a selected time interval. However, such generality does not give much physical insight into the field dynamics and underlying mechanisms. Consequently, we focus on the properties of fields at only two times. These are determined from the joint probability distribution $Q(\vec{\mathcal{E}},t|\vec{\mathcal{E}}',t')$ for the probability density to find the field value $\vec{\mathcal{E}}$ at time t and the value $\vec{\mathcal{E}}'$ at time t'. A more transparent derived property is the conditional electric field $\vec{\mathcal{E}}(t|\vec{\mathcal{E}}_0)$, giving the average field at time t after an observed value of $\vec{\mathcal{E}}_0$. As indicated in Sec. III, this describes the nonlinear response of the electric field to arbitrary initial distributions of the field. The conditional electric field is the primary property studied in detail here.

In Sec. II the distributions for fields at one and two times are given and some known results for the idealized model are recalled (the Holtsmark distribution, the distribution of field derivatives, and the field autocorrelation function). These results are compared with those from molecular dynamics simulation (including interactions) for screened Coulomb fields at several values of the plasma coupling, illustrating the accuracy and the relevance of the model. In Sec. III the conditional electric field is calculated. The results are illustrated over a range of plasma coupling as a function of time, screened length, and initial field value. The theoretical conditional electric field is compared with molecular dynamics simulation results, again showing good agreement.

All theoretical calculations for the model here are exact and therefore provide a critical test for approximate stochastic representations of the electric field. The most complete representation currently available considers the electric field as a stochastic variable governed by a kangaroo process [7]. An important feature of this process is the possibility to imbed in it the known exact stationary field distribution and electric field autocorrelation function. The conditional electric field then can be calculated and compared to the exact value obtained here, as a test of this parametrization of the kangaroo process. This is done in Sec. IV, where it is shown that the kangaroo process gives a poor approximation on all time scales, and the reasons for this failure are discussed. A possible alternative approximation for the joint probability density is proposed and criticized. The primary results presented here are summarized and discussed in Sec. V.

II. DEFINITIONS AND RELATIONSHIPS

A. General definitions

Before introducing our model, the properties of interest are defined for a one-component plasma (OCP) of N ions with mass m and charge Ze, interacting via Coulomb or screened Coulomb forces in a uniform neutralizing background. Most of the definitions below apply as well for more complex plasmas, with obvious changes. The electric field at a neutral point (chosen to be the origin) due to the OCP is given by

$$\vec{E} \equiv \sum_i^N \vec{e}(\vec{q}_i),\ \vec{e}(\vec{r}) \equiv Ze\hat{\vec{r}}(1+\alpha r)e^{-\alpha r}r^{-2} + \vec{e}_b, \quad (1)$$

where N is the number of ions, α is the inverse screening length, $\hat{\vec{r}} = \vec{r}/r$, and $\vec{e}(\vec{q}_i)$ is the electric field due to the ith particle plus a contribution from the uniform background $\vec{E}_b = N\vec{e}_b$. The probability density for field values $Q(\vec{\epsilon})$ is

$$Q(\vec{\epsilon}) = \left\langle \delta(\vec{\epsilon} - \vec{E}(t)) \right\rangle = (2\pi)^{-3} \int d\lambda e^{-i\vec{\lambda}\vec{\epsilon}} e^{G(\lambda)}. \quad (2)$$

The second equality defines the associated generating function $G(\lambda)$,

$$G(\lambda) = \ln\left(\left\langle e^{i\vec{\lambda}\cdot\vec{E}(t)} \right\rangle \right). \quad (3)$$

In all of the following it is understood that the angular brackets represent a Gibbs ensemble average, so that only equilibrium states are considered. Then from time translational invariance of the Gibbs ensemble it follows that (2) is a time-independent stationary distribution.

Dynamic properties at two times, the smaller of which is chosen to be zero by time translational invariance, are determined from the joint distribution for a field value $\vec{\epsilon}$ at time t [8],

$$Q(\vec{\epsilon},t;\vec{\epsilon}',0) = \left\langle \delta(\vec{\epsilon} - \vec{E}(t))\delta(\vec{\epsilon}' - \vec{E}) \right\rangle$$
$$= (2\pi)^{-6} \int d\lambda d\lambda' e^{-i\vec{\lambda}\vec{\epsilon} - i\vec{\lambda}'\vec{\epsilon}'} e^{G(\vec{\lambda}\vec{\lambda}';t)}. \quad (4)$$

The generating function in this case is given by

$$G(\vec{\lambda},\vec{\lambda}';t)=\ln\left(\left\langle e^{i\lambda\cdot\vec{E}(t)}e^{i\lambda'\cdot\vec{E}}\right\rangle\right). \tag{5}$$

The initial and the final values for $Q(\vec{\epsilon},t;\vec{\epsilon}',0)$ and $G(\vec{\lambda},\vec{\lambda}')$ are easily determined to be

$$Q(\vec{\epsilon},0;\vec{\epsilon}',0)=\delta(\vec{\epsilon}-\vec{\epsilon}')Q(\vec{\epsilon}'),\ Q(\vec{\epsilon},\infty;\vec{\epsilon}',0)=Q(\vec{\epsilon})Q(\vec{\epsilon}'), \tag{6}$$

$$G(\vec{\lambda},\vec{\lambda}';0)=G(|\vec{\lambda}+\vec{\lambda}'|),\ G(\vec{\lambda},\vec{\lambda}';\infty)=G(\vec{\lambda})+G(\vec{\lambda}'). \tag{7}$$

The generating functions have been introduced because they are the more convenient objects for analysis by both simulation and analytic methods. Several important properties are directly derived from $G(\vec{\lambda},\vec{\lambda}';t)$. The time independent distribution of electric field derivatives

$$P(\vec{\eta})\equiv\left\langle\delta(\vec{\eta}-\dot{\vec{E}})\right\rangle,\quad \dot{\vec{E}}\equiv\left(\frac{d}{dt}\vec{E}(t)\right)_{t=0} \tag{8}$$

can be calculated from $G(\vec{\lambda},\vec{\lambda}';t)$ according to [9]

$$P(\vec{\eta})=(2\pi)^{-3}\int d\vec{\lambda}e^{-i\vec{\lambda}\cdot\vec{\eta}}e^{J(\lambda)},$$
$$J(\lambda)=\lim_{t\to 0}G\left(\frac{\vec{\lambda}}{t},-\frac{\vec{\lambda}}{t};t\right). \tag{9}$$

The statistical properties of field dynamics at short times is determined by the time independent distributions $Q(\vec{\epsilon})$ and $P(\vec{\eta})$ for the first two coefficients in a Taylor series expansion of any function of $\vec{E}(t)$. The simplest measure of longer time properties is given by the electric field autocorrelation function $C(t)$,

$$C(t)\equiv\langle\vec{E}(t)\cdot\vec{E}\rangle=-\left(\frac{\partial^2}{\partial\lambda_i\partial\lambda_i'}G(\vec{\lambda},\vec{\lambda}';t)\right)_{\lambda=\lambda'=0}. \tag{10}$$

A considerably more detailed description of the field dynamics at all times is given by the conditional average of the electric field

$$\mathcal{E}_i(t\,|\,\vec{\epsilon})\equiv\langle E_i(t)\delta(\vec{\epsilon}-\vec{E})\rangle/\langle\delta(\vec{\epsilon}-\vec{E})\rangle \tag{11}$$
$$=Q^{-1}(\epsilon)(2\pi)^{-3}\int d\vec{\lambda}e^{-i\vec{\lambda}\cdot\vec{\epsilon}+G(\lambda)}\times\left(-i\frac{\partial}{\partial\lambda_i'}G(\vec{\lambda}',\vec{\lambda};t)\right)_{\vec{\lambda}'=0}. \tag{12}$$

All of the above expressions are formally exact. There are practical and accurate methods to calculate the generating function $G(\lambda)$ for the static field distribution [10]. The generating function $G(\vec{\lambda},\vec{\lambda}';t)$ has been studied recently in a number of limits [8,11] and by semiphenomenological models [9], but much less is known about these dynamical properties. Indeed, one motivation for our detailed study of the idealized plasma below is to expose more completely some of these properties.

B. Noninteracting plasma model

The charged particles of the OCP generate not only the electric field (1) at the neutral point, but also similar fields at each of the other charges. The latter couples the dynamics of all particles. We consider now a model in which all fields are neglected except those at the neutral point—only the test particle detects the charge on the plasma constituents. The justification for this model lies in the fact that each particle experiences a superposition of fields from all other particles (due to the long range nature of the interaction), whose collective effect yields small velocity changes relative to the thermal velocity. The resulting trajectories are then approximately straight lines, as for a noninteracting system. This is observed in molecular dynamics simulations, with occasional larger velocity changes due to very close encounters. This qualitative picture is supported by direct observation of trajectories in the molecular dynamics simulations described below.

The generating functions $G(\vec{\lambda})$ and $G(\vec{\lambda},\vec{\lambda}';t)$ at a neutral point for noninteracting particles can be calculated exactly (see Appendix A)

$$G(\lambda)=n\int d\vec{r}\left(e^{i\vec{\lambda}\cdot\vec{e}(\vec{r})}-1\right), \tag{13}$$

$$G(\vec{\lambda},\vec{\lambda}';t)=n\int d\vec{r}d\vec{v}\phi(v)\left(e^{i[\vec{\lambda}\cdot\vec{e}(\vec{r}+\vec{v}t)+\vec{\lambda}'\cdot\vec{e}(\vec{r})]}-1\right), \tag{14}$$

where $\phi(v)$ is the Maxwell-Boltzmann distribution and n is the number density. *For the special case of Coulomb fields* exact scaling relations are obtained directly from (13) and (14),

$$G(\lambda)=a^{-3}G(a^2\lambda),\ G(\vec{\lambda},\vec{\lambda}';t)=a^{-3}G(a^2\vec{\lambda},a^2\vec{\lambda}';at). \tag{15}$$

The generating functions $G(\lambda)$, $J(\lambda)$, and the correlation function $C(t)$ can be calculated analytically for this case with the results

$$G(\lambda)=-\frac{2}{5}(2\pi)^{1/2}(\lambda e_0)^{3/2}, \tag{16}$$

$$J(\lambda)=\frac{\sqrt{\pi}}{2}\left[1+(2\sqrt{3})^{-1}\sinh^{-1}(\sqrt{3})\right](e_0/t_0)\lambda, \tag{17}$$

$$C(t)=e_0^2(6/\sqrt{\pi})(t_0/t), \tag{18}$$

where $e_0\equiv Ze/r_0^2$ is the single-particle field at the average particle distance r_0, defined by $4\pi nr_0^3/3\equiv 1$, and $t_0\equiv r_0/u$ is the time to cross this distance at the thermal velocity $u\equiv(2k_BT/m)^{1/2}$. The short and the long time behavior of $G(\vec{\lambda},\vec{\lambda}';t)$ for Coulomb fields can also be obtained,

$$G(\vec{\lambda},\vec{\lambda}';t) \to G(|\vec{\lambda}+\vec{\lambda}'|) - (t/t_0)^2 c_0(\lambda\lambda')^2(1-x^2) \times |\vec{\lambda}+\vec{\lambda}'|^{-7/2} + \cdots , \quad (19)$$

$$G(\vec{\lambda},\vec{\lambda}';t) \to G(\lambda) + G(\lambda') + (t_0/t)^3 c_\infty G(\lambda)G(\lambda') + \cdots , \quad (20)$$

with $c_0 \equiv 9(2\pi e_0)^{1/2}/16, c_\infty \equiv (4/3\sqrt{\pi})$, and $x = \cos(\hat{\vec{\lambda}}\cdot\hat{\vec{\lambda}}')$.

For screened Coulomb fields no such simplifications occur. Further analytic simplification of (13) and (14) is possible, although, in general, numerical methods are required to evaluate these expressions or those derived from them. Practical expressions for the numerical evaluation of the field distribution $Q(\vec{\epsilon})$, the distribution of field derivatives $P(\vec{\eta})$, and the electric field autocorrelation function $C(t)$ are given in Appendix B. In the remainder of this section we compare the results from these expressions to those from molecular dynamics simulations for the same fields *and* with interactions among the plasma particles via the potential from which the field is derived. The simulations were performed only for screened interactions, using periodic boundary conditions for system dimensions large compared to the screening length. A natural consequence of the use of periodic boundary conditions is the introduction of the "minimum image convention" [12], which ensures that the interaction volume is centered on the particle on which we calculate the force. The molecular dynamics technique has been used extensively in the past for studying the statistical properties of moderately to strongly coupled plasmas [12]. We have used a standard molecular dynamics simulation for computing the field distribution, the distribution of field derivatives, the electric field autocorrelation function, and the conditional electric field. Instead of the plasma parameter Γ, it is instructive to characterize the coupling in terms of the number of particles in a Debye sphere $N_D \equiv 4\pi n\lambda_D^3/3$, where $\lambda_D \equiv (k_B T/4\pi n Z^2 e^2)^{1/2}$ is the Debye length. Note that $\gamma \equiv N_D^{-1} = (r_0/\lambda_D)^3$ is an alternative measure of the plasma coupling strength. It follows from spherical symmetry that $Q(\vec{\epsilon})$ and $P(\vec{\eta})$ depend only on the magnitudes ϵ and η, respectively. The distributions for these magnitudes are defined by

$$4\pi\epsilon^2 Q(\vec{\epsilon}) \equiv q(\epsilon), \qquad 4\pi\eta^2 P(\vec{\eta}) \equiv p(\eta). \quad (21)$$

In Fig. 1 the electric field distribution obtained from our

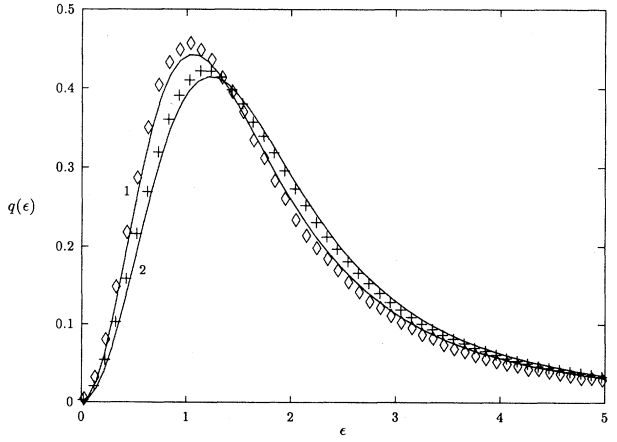

FIG. 1. Probability density $q(\epsilon)$ for the electric field magnitudes in units of e_0 at $N_D = 8$ (curve 1) and $N_D = 27$ (curve 2); also shown are the corresponding results from molecular dynamics.

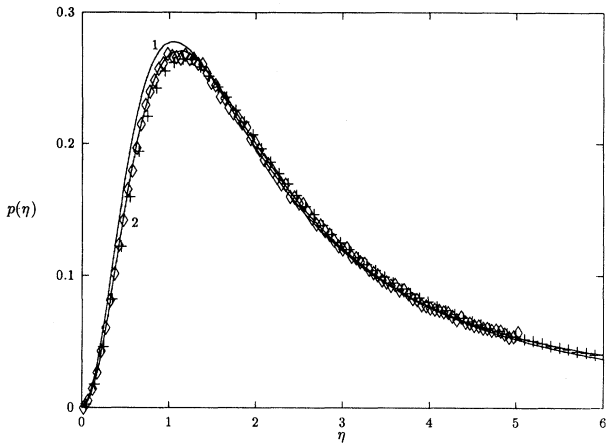

FIG. 2. Probability density $p(\eta)$ for the electric field derivative magnitudes in units of $e_0 u/r_0$; same conditions as Fig. 1.

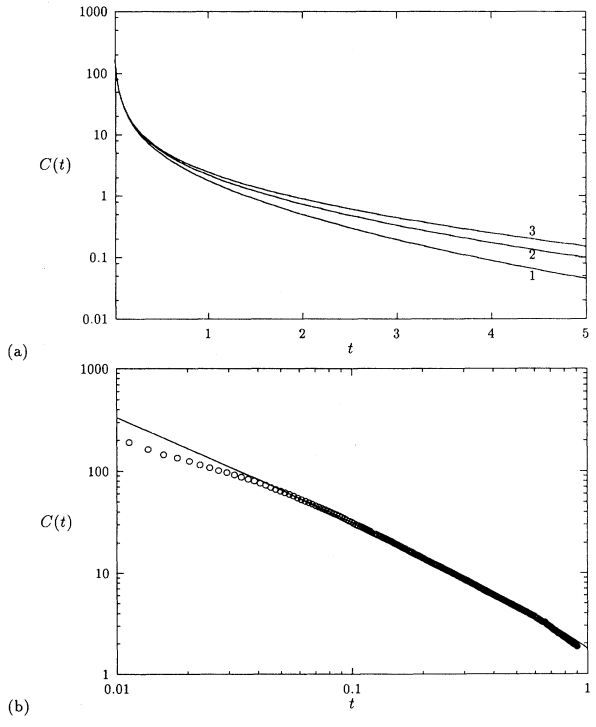

FIG. 3. Electric field autocorrelation function $C(t)$ in units of e_0^2, with t in units of r_0/u. (a) shows the theoretical result at $N_D = 8$ (curve 1), $N_D = 27$ (curve 2), and $N_D = 64$ (curve 3). (b) shows a comparison with results from molecular dynamics simulation at $N_D = 8$.

model is compared to results from the simulation for the two cases of $N_D = 8$ and 27 particles per Debye sphere. In both cases, relatively good agreement is observed. A similar quantitative agreement is found in Fig. 2 for the comparison of the field derivatives. The field autocorrelation function $C(t)$ obtained for the model is shown in Fig. 3(a) for the three cases of $N_D = 8, 27$, and 64. At short times all behave as $1/t$, while the effects of screening are evident for times greater than 0.5. The comparison with simulation results are shown in Fig. 3(b) for $N_D = 8$. For $t < 0.5$ the effects of interactions are negligible and the model should agree well with the simulation results. The significant differences observed at short times is due to errors in simulation data at large values for $C(t)$. For later times this is not a problem and the simulation predicts a slightly faster decorrelation than the model, due to interactions. This interpretation has been confirmed by performing simulations without interactions among the particles as well. The primary conclusion from these illustrations is that the idealized model is in quantitative agreement with the simulation results for real plasmas, justifying the following more complete picture of the field dynamics.

III. CONDITIONAL ELECTRIC FIELD DYNAMICS

The conditional electric field is defined by Eq. (11). To interpret this expression, note first that the initial value is $\vec{\mathcal{E}}(0 \mid \vec{\epsilon}) = \vec{\epsilon}$ so that $\vec{\mathcal{E}}(t \mid \vec{\epsilon})$ is the subsequent value of the average field following a specified initial value. It can be understood also as the nonlinear response function for the electric field. To see this, consider a perturbation of the Hamiltonian to $H' = H + \vec{\lambda} \cdot \vec{E}$. Then the average electric field at time t for an initial Gibbs ensemble with Hamiltonian H' is

$$\langle \vec{E}(t) \rangle_\lambda \equiv \left\langle \vec{E}(t) e^{-\beta \vec{\lambda} \cdot \vec{E}} \right\rangle \Big/ \left\langle e^{-\beta \vec{\lambda} \cdot \vec{E}} \right\rangle = \int d\vec{\epsilon} \vec{\mathcal{E}}(t \mid \vec{\epsilon}) Q(\vec{\epsilon}, \vec{\lambda}), \tag{22}$$

$$Q(\vec{\epsilon}, \vec{\lambda}) \equiv Q(\epsilon) e^{-\beta \vec{\lambda} \cdot \vec{\epsilon}} / \langle e^{-\beta \vec{\lambda} \cdot \vec{E}} \rangle. \tag{23}$$

$Q(\vec{\epsilon}, \vec{\lambda})$ is the normalized initial distribution of field values for the Gibbs ensemble with Hamiltonian H'. An expansion of (22) in powers of $\vec{\lambda}$ gives a series whose time dependent coefficients are the response functions. The coefficient of first order in $\vec{\lambda}$ is the linear response function $C(t)$ of Eq. (10). The higher-order coefficients define the nonlinear response functions as the moments of $\vec{\mathcal{E}}(t \mid \vec{\epsilon})$ with respect to $\vec{\epsilon}$. Since $\vec{\mathcal{E}}(t \mid \vec{\epsilon})$ determines all of these functions it will be referred to as the nonlinear response function.

The calculation of $\vec{\mathcal{E}}(t \mid \vec{\epsilon})$ from Eqs. (12) and (14) is outlined in Appendix B. It follows from rotational invariance of the ensemble that $\vec{\mathcal{E}}(t \mid \vec{\epsilon})$ is proportional to $\vec{\epsilon}$ and it is sufficient to study the scalar function $C(t \mid \epsilon)$ defined by

$$\vec{\mathcal{E}}(t \mid \vec{\epsilon}) \equiv C(t \mid \epsilon) \vec{\epsilon} \tag{24}$$

with the initial condition $C(0 \mid \epsilon) = 1$. The following results are based on direct numerical evaluation of the integral representation Eq. (B14). All fields are measured relative to e_0 and the time is relative to r_0/u. Consider first the case of Coulomb fields. There is no intrinsic dependence on coupling strength for this case, so only the dependence of $C(t \mid \epsilon)$ on t and ϵ is relevant. Figure 4 shows the time dependence for $\epsilon = 0.2, 1.0$, and 5.0. The interesting qualitative features are (i) a monotone decay in time on a time scale that decreases with increasing ϵ, (ii) a long time decay that behaves asymptotically as t^{-1}, and (iii) a short time domain of very slow decay. The inverse dependence of the time scale on ϵ can be understood by assuming that the entire field at the neutral point is due to a single particle, initially at a distance $R(\epsilon) = (Ze/\epsilon)^{1/2}$. The time scale for decay of the initial field can be estimated by the average time to cross a sphere of this radius $T(\epsilon) = R(\epsilon)/u$, which decreases with increasing ϵ. It also gives an estimate for the initial short time persistence of the initial field value. The conditional electric field for this single-particle model is calculated in Appendix C. However, this single-particle picture does not apply for small initial fields where comparable contributions from many particles occur.

The case of screened fields is qualitatively similar with some notable differences. Figure 5 shows $C(t \mid \epsilon)$ as a function of the screening parameter α [see Eq. (1)], for $\epsilon = 0.2, 1$, and 5. For screening lengths of the order of r_0 (i.e., $\alpha \sim 1$) there is a significant enhancement over the initial field value for short times. This qualitative behavior is present for all screening lengths, although it decreases with increasing screening length and increasing field values. A second qualitative difference is the faster decay in time for increased screening lengths. These features also can be interpreted via the single-particle field model. The distance $R(\epsilon)$ of the single particle is now determined from

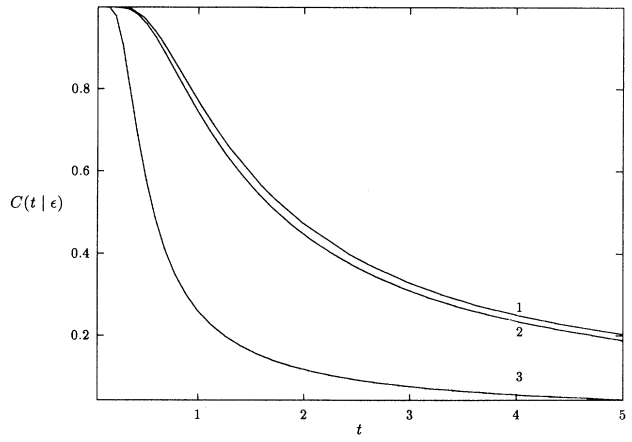

FIG. 4. Conditional electric field $C(t \mid \epsilon)$ as a function of time t for Coulomb fields at $\epsilon = 0.2$ (curve 1), $\epsilon = 1$ (curve 2), and $\epsilon = 5$ (curve 3).

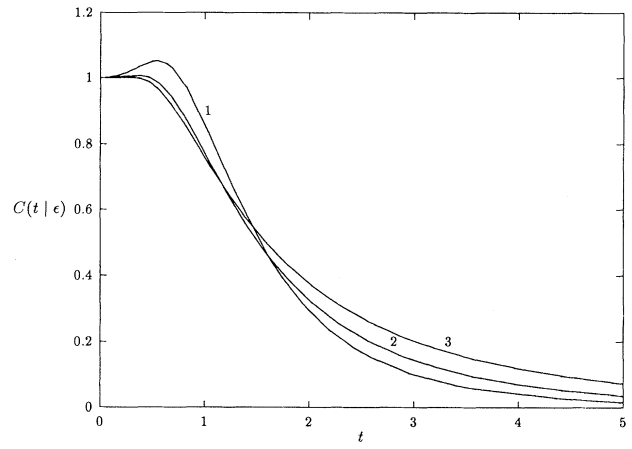

FIG. 5. Same as Fig. 4 at $\epsilon = 0.2$, but now for screened fields with screening parameter $\alpha = 1$ (curve 1), $\alpha = 0.5$ (curve 2), and $\alpha = 0.25$ (curve 3).

$$\epsilon = Ze(1 + \alpha R)e^{-\alpha R}R^{-2}. \tag{25}$$

It is easily seen that the associated time scale $T(\epsilon) = R(\epsilon)/u$ is always smaller than that for $\alpha = 0$ and the short time persistence period is longer. Also, for small initial fields, $\alpha R > 1$ and the field increases (decreases) exponentially if the particle is directed toward (away from) the neutral point. The net result is an enhanced field over the time interval $T(\epsilon)$. The longer time decay is faster once the particle is moving away from the neutral point since the value of the screened field for given distance $r(t)$ is smaller.

The asymptotic short and long time behavior can be determined in the case of Coulomb fields

$$C(t \mid \epsilon) = \begin{cases} D_1(\epsilon)/t, & t/t_0 \gg 1 \\ 1 - D_2(\epsilon)t^9, & t/t_0 \ll 1. \end{cases} \tag{26}$$

The functions $D_1(\epsilon)$ and $D_2(\epsilon)$ have complicated analytic structure and their detailed form will not be given here. We note only the qualitative behavior $D_1(\epsilon) \sim \epsilon$ for $\epsilon/e_0 \ll 1$ and $D_2(\epsilon) \sim \epsilon^{-1}$ for $\epsilon/e_0 \gg 1$. In the case of screened Coulomb fields the long time decay of $C(t \mid \epsilon)$ is much faster than in (26), with the limiting form $C(t \mid \epsilon) \sim t^{-5}$. This implies that the asymptotic form (26) is not approached uniformly with respect to the field value ϵ.

Finally, we compare the exact conditional electric field for our model with molecular dynamics simulations that include particle interactions. Figures 6 and 7 show the results for $\epsilon = 1$ and 4 at $N_D = 8$ and 27. In all cases the screening length is $\alpha^{-1} = \lambda_D$. The molecular dynamics (MD) results have been obtained through a process providing independent realizations of microfields measured at neutral points. The selection of the statistical sample is monitored by testing the initial field strengths such as $e = 1.00 \pm 0.02$ or $e = 4.00 \pm 0.02$. From a statistical point of view, the narrow interval used for the selection ensures the good resolution needed to compare MD with analytical results. However, considering a small set of independent realizations slows down the averaging process. Therefore, some noise could not be completely removed from the MD results. A few simulated data points keep track of strong collisional events between charged and neutral points that have not been averaged out. Nevertheless, the statistical distribution of the MD data set

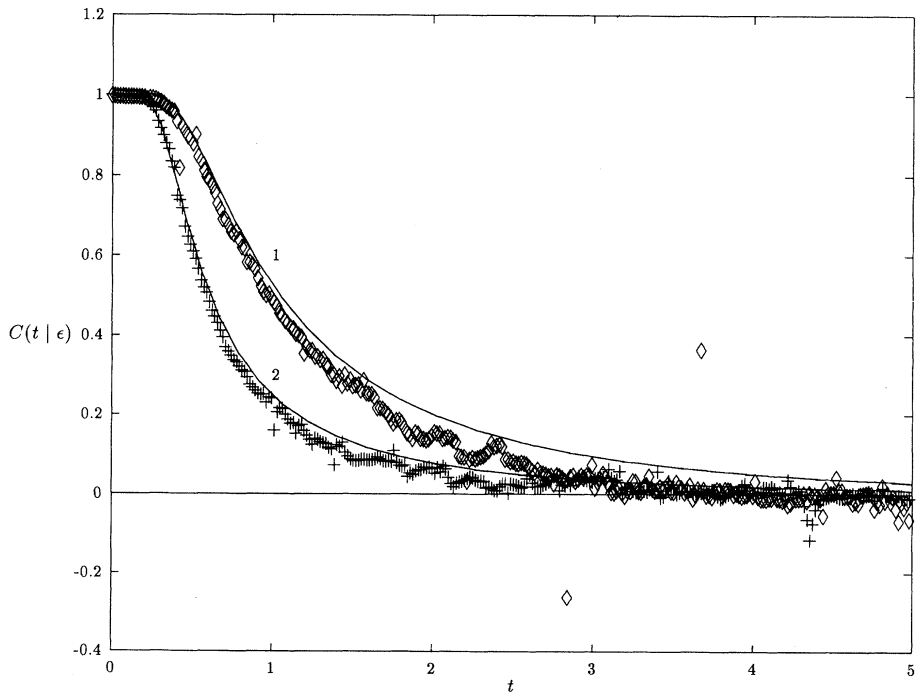

FIG. 6. Comparison of the conditional electric field $C(t \mid \epsilon)$ with results from molecular dynamics simulation for $N_D = 27$ at $\epsilon = 1$ (curve 1) and $\epsilon = 4$ (curve 2).

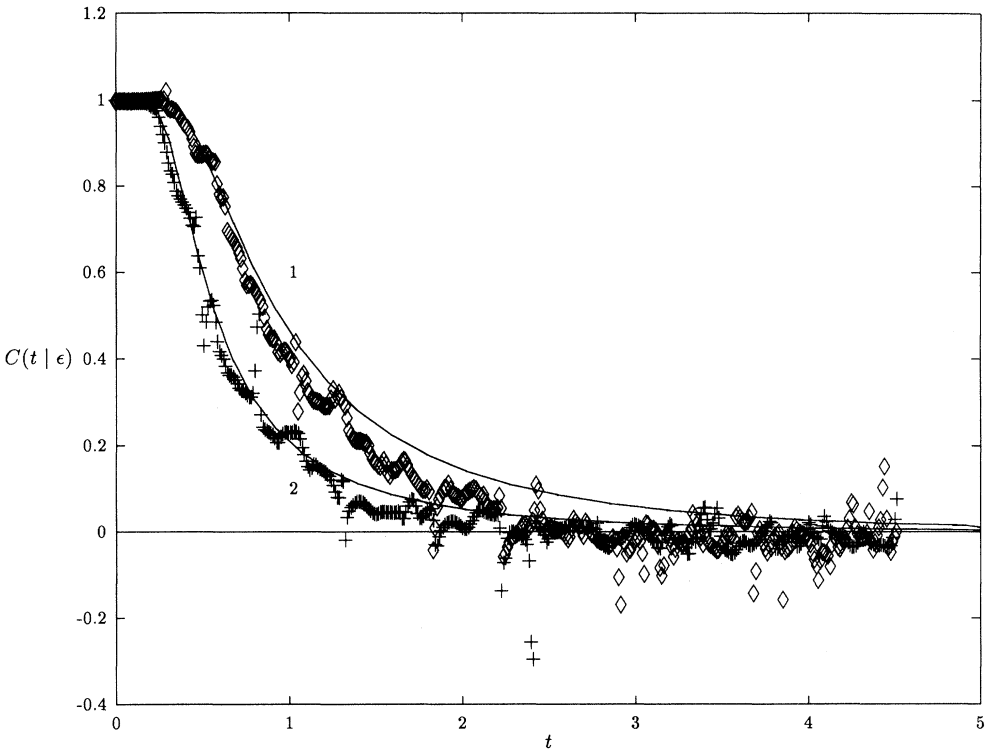

FIG. 7. Same as Fig. 6, but for $N_D = 8$.

is good enough to provide a basis of comparisons with the theoretical model. Again in this case the simulations performed without interactions among charged particles are in good agreement with the model, confirming that molecular dynamics with interactions predicts a faster decorrelations for the conditional electric field.

IV. STOCHASTIC FIELD MODELS

The microscopic dynamics of the electric field is determined from the detailed dynamics of all particles in the plasma. The large number of particles then leads to a rapidly varying and highly irregular time dependence for the fields. This suggests the possibility of modeling the field dynamics as some smooth regular behavior (reflected in the average dynamics) with random noise superimposed on it. There are methods of nonequilibrium statistical mechanics that allow formulation of the problem in this way, with the field treated as a stochastic variable. The problem then is to determine the regular behavior and to characterize the noise from the underlying microscopic dynamics. Alternatively, a purely phenomenological approach can be taken whereby a particular stochastic process is assumed for convenience and practicality. The most widely used process in the present context is the kangaroo process [2]. It is a Markovian process so that all multitime properties are determined from the joint distribution function $Q(\vec{\epsilon}, t; \vec{\epsilon}', t')$, which obeys the equation

$$\left(\frac{\partial}{\partial t} + \nu(\epsilon)\right) Q(\vec{\epsilon}, t, \vec{\epsilon}', t') = \nu(\epsilon) Q(\vec{\epsilon}) \int d\vec{\epsilon}'' \overline{\nu}(\epsilon'') Q(\vec{\epsilon}'', t; \vec{\epsilon}', t'). \quad (27)$$

Here $\nu(\epsilon)$ is a function of the field magnitude to be determined and $\overline{\nu}(\epsilon)$ is defined by

$$\overline{\nu}(\epsilon) \equiv \nu(\epsilon) \Big/ \int d\vec{\epsilon}' \nu(\epsilon') Q(\vec{\epsilon}'). \quad (28)$$

It is easily verified that $Q(\vec{\epsilon})Q(\vec{\epsilon}')$ is the long time, stationary solution to (27). An integral equation representation is obtained directly by integration (for $t \geq t'$)

$$Q(\vec{\epsilon}, t, \vec{\epsilon}', t') = e^{-\nu(\epsilon)(t-t')} \delta(\vec{\epsilon} - \vec{\epsilon}') Q(\vec{\epsilon}') + \int_{t'}^{t} d\tau e^{-\nu(\epsilon)(t-\tau)} \nu(\epsilon) Q(\vec{\epsilon}) d\vec{\epsilon}'' \times \overline{\nu}(\epsilon'') Q(\vec{\epsilon}'', \tau; \vec{\epsilon}', t'), \quad (29)$$

where the initial condition (6) has been used.

The correlation function $C(t)$ can be calculated from (29) as a function of $\nu(\epsilon)$,

$$C(t) = \int d\vec{\epsilon} d\vec{\epsilon}' \vec{\epsilon} \cdot \vec{\epsilon}' Q(\vec{\epsilon}, t, \vec{\epsilon}', 0) = \int d\vec{\epsilon} \epsilon^2 Q(\vec{\epsilon}) e^{-\nu(\epsilon)t} \quad (30)$$

[the second term of (29) does not contribute due to spherical symmetry]. The right-hand side is a positive function

of t. It is possible to show [2] that $\nu(\epsilon)$ can be chosen to yield any given positive function $C(t)$. In Appendix D we sketch a procedure of finding $\nu(\epsilon)$ [2,7]. Thus the kangaroo process is characterized by two arbitrary functions $Q(\vec{\epsilon})$ and $\nu(\epsilon)$, which can be chosen to yield the exact stationary distribution and the field correlation function known from statistical mechanics. Of course, this does not ensure that other properties are given correctly.

To explore this last point, the conditional electric field can be calculated from (29) and compared to the exact result of Sec. III. The conditional electric field for the kangaroo process is found to be

$$\vec{\mathcal{E}}(t\,|\,\vec{\epsilon}) = \int d\vec{\epsilon}'\,\vec{\epsilon}'\,Q(\vec{\epsilon}',t,\vec{\epsilon},0)/Q(\vec{\epsilon}) = e^{-\nu(\epsilon)t}\vec{\epsilon}. \tag{31}$$

Again, the second term of (29) does not contribute. Equivalently, $C(t|\epsilon)$ is a simple exponential function for all time. This is clearly in contradiction to the exact result of Sec. III for Coulomb fields, where a crossover from almost constant behavior at short times to t^{-1} behavior at long times is found. The kangaroo process is never a good approximation in this case. For screened fields, the short time enhancement of Figs. 6 and 7 cannot be reproduced by the kangaroo process, which leads to monotonic decay. This is illustrated in Fig. 8 for $\alpha = \epsilon = 1$.

It appears from these results that the successful applications of the kangaroo process to calculate spectral line profiles must be due to its primary dependence on electric fields only through $Q(\vec{\epsilon})$ and $C(t)$. The former provides a description of the initial fields before radiation, while the latter gives the correlation time. Evidently this is sufficient in many cases. For properties sensitive to other field characteristics, the results of this section indicate that the kangaroo process should not be used.

A primary advantage of the kangaroo process is its simplicity. It would be useful to have an alternative stochastic process that allows modeling of $Q(\vec{\epsilon}), C(t)$, *and* $C(t\,|\,\epsilon)$ with the same relative simplicity of the kangaroo process.

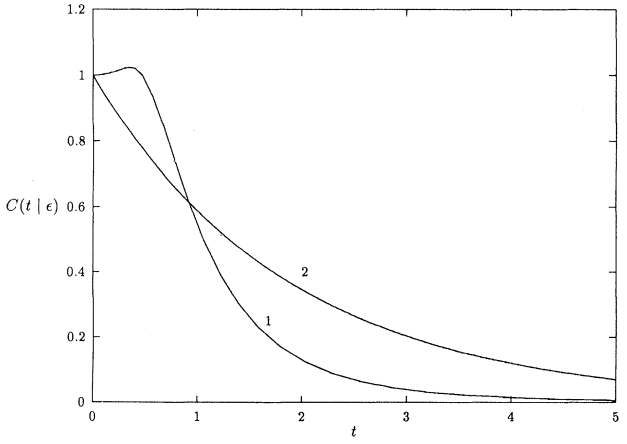

FIG. 8. Conditional electric field $C(t\,|\,\epsilon)$ at $\epsilon = 1$ and screening length $\alpha = 1$: exact (curve 1) and from Eq. (31) (curve 2).

In this spirit we consider a suggestion of Ref. [6] for an approximation to the joint distribution

$$Q(\vec{\epsilon},t,\vec{\epsilon}',0) = \alpha^{-3}(t\,|\,\epsilon')Q([\vec{\epsilon} - \vec{\mathcal{E}}(t\,|\,\vec{\epsilon}')]/\alpha(t\,|\,\epsilon'))Q(\vec{\epsilon}'). \tag{32}$$

This gives the exact conditional electric field $\vec{\mathcal{E}}(t\,|\,\vec{\epsilon}')$ and consequently $C(t)$ as well. To obtain the correct long time stationary solution and the correct initial values of (6), the function $\alpha(t\,|\,\epsilon')$ must have the properties

$$\alpha(0\,|\,\epsilon') = 0, \qquad \alpha(\infty\,|\,\epsilon') = 1. \tag{33}$$

Otherwise it can be chosen arbitrarily. This parameter effectively gives the time scale for the transition to the equilibrium state. A physically reasonable and simple choice is

$$\alpha(t\,|\,\epsilon) = \{1 - \exp[-2\nu(\epsilon)t]\}^{1/2}, \tag{34}$$

where $\nu(\epsilon)$ is determined from the definition (30).

With this form, (32), (34), and (30) become exact for the special case $\nu(\epsilon)$ =const and the process is assumed to be Gaussian-Markovian. The present results are a plausible extrapolation of this functional form to the case of field dependent $\nu(\epsilon)$.

With the quantities $Q(\vec{\epsilon}), C(t)$, and $C(t\,|\,\vec{\epsilon})$ known exactly from the statistical mechanics for the system of noninteracting particles, they can be used to determine (32) and (34) with no free parameters. The result provides a practical means to study any two time property involving electric field dynamics at a neutral point. We intend to compare the predictions of this model with computer simulations of $Q(\vec{\epsilon},t,\vec{\epsilon}',0)$ in a future investigation. An important shortcoming, however, is that (32) does not appear to be associated with any Markovian process so it provides no insight into multitime field dynamics.

V. DISCUSSION

The idealized model for electric field dynamics presented here is sufficiently simple that any desired property can be reduced to quadratures. This has been illustrated for the conditional electric field that characterizes the nonlinear response of the field to an arbitrary initial value. The results for this model constitute the only information presently available about electric field dynamics beyond linear response, firmly based in statistical mechanics. Furthermore, it has been demonstrated that the idealization of independent particles does not prohibit extrapolation of the properties for this model to those for real plasmas with interactions. The limited comparisons with computer simulation presented here indicate quantitative agreement in all cases considered, over a range of plasma coupling strengths.

An important application of electric field dynamics is to atomic radiation problems, where the variation of the field over the time for emission or absorption of a photon determines the spectral line shape. The conditional electric field provides the relevant information for this

variation and indicates different characteristic correlation times for each initial field. In principle, the line profile can be calculated for each chosen initial field followed by an average of the profiles over the ensemble for initial fields. This is an example of a highly nonlinear dependence on the field dynamics that is not captured by the field autocorrelation function. Furthermore, the results of Sec. III show the decay of the initial field can be quite complicated, with very slow decay at short times and algebraic decay at longer times; it is never well approximated by simple exponential decay with a single characteristic time.

The model admits an exact analysis and therefore provides a benchmark for comparison of more realistic, but approximate, many-body methods. It is also important for testing stochastic models for electric field dynamics. As an example of this, we have shown in Sec. IV that the kangaroo process does not lead to a realistic conditional electric field even though it uses the exact stationary distribution and field covariance. Stochastic models are very useful for complex applications and as a way of extracting only the relevant physics. It is an interesting question as to whether a sufficiently simple Markovian process can be constructed that represents well the statistical mechanics of the independent particle model. The discussion here has been limited to electric fields at neutral points. Its relative success suggests consideration of the same model for fields at a charged point. The only difference is that the trajectories become hyperbolas rather than straight lines. This poses no serious complication in the analysis and we plan to present the corresponding results in a future paper.

ACKNOWLEDGMENTS

The research of J.W.D. and M.B. was supported by National Science Foundation Grant No. PHY 9312723. Also J.W.D. is grateful to the Universite de Provence for its support and hospitality.

APPENDIX A: STATISTICAL MECHANICS

Any property depending on the electric field $\vec{E}(t)$ history for the time interval $0 \le t \le T$ can be calculated from the generating functional $G[\vec{\lambda}]$ defined by

$$\exp(G[\vec{\lambda}]) = \left\langle \exp\left(i \int_0^T dt \vec{\lambda}(t) \cdot \vec{E}(t) \right) \right\rangle , \tag{A1}$$

where $\vec{\lambda}(t)$ is a test function and $\vec{E}(t)$ is the microsopic electric field defined in (1). The angular brackets denote an ensemble average

$$\langle Y \rangle \equiv \int dx_1 \cdots dx_N Y(x_1, ..., x_N) \rho(x_1, ..., x_N). \tag{A2}$$

Here $x_i = \{\vec{r}_i, \vec{v}_i\}$ denotes both the position and the velocity of the ith particle at $t = 0$ and $\rho(x_1, ..., x_N)$ is the probability density for the microscopic state $\{x_1, ..., x_N\}$. For the system of noninteracting particles considered here it is taken to be of a product form (no initial correlations)

$$\rho(x_1, ..., x_N) = \prod_{i=1}^{N} \rho(x_i), \qquad \int dx_i \rho(x_i) = 1. \tag{A3}$$

All multitime correlation functions can be calculated from (A1) by suitable functional differentiation

$$\left. \frac{\delta G[\vec{\lambda}]}{\delta \lambda_{\alpha_1}(t_1) \cdots \delta \lambda_{\alpha_m}(t_m)} \right|_{\lambda=0} = \langle \delta E_{\alpha_1}(t_1) \cdots \delta E_{\alpha_m}(t_m) \rangle . \tag{A4}$$

More generally, the average of *any* functional of the electric field $\langle F[\vec{E}] \rangle$ can be determined by functional Fourier transformation of $\exp\{G[\vec{\lambda}]\}$. In this appendix it is shown that the calculation of $G[\lambda]$ for any state of the form (A3) can be reduced to a one-particle average.

The electric field in (A1) has the form

$$\vec{E}(t) = \sum_{i=1}^{N} \vec{e}(\vec{r}_i(t)) = \sum_{i=1}^{N} \vec{e}(\vec{r}_i + \vec{v}_i t), \tag{A5}$$

so that (A1) reduces to

$$\begin{aligned} \exp\{G[\vec{\lambda}]\} &= \prod_{i=1}^{N} \int dx_i \exp\left(i \int_0^T dt \vec{\lambda}(t) \cdot \vec{e}_i(\vec{r}_i(t)) \right) \rho(x_i) \\ &= \prod_{i=1}^{N} \left\{ 1 + \int dx_i \left[\exp\left(i \int_0^T dt \vec{\lambda}(t) \cdot \vec{e}_i(\vec{r}_i(t)) \right) - 1 \right] \rho(x_i) \right\} \\ &= \left\{ 1 + N^{-1} N \int dx \left[\exp\left(i \int_0^T dt \vec{\lambda}(t) \cdot \vec{e}(\vec{r}(t)) \right) - 1 \right] \rho(x) \right\}^N \\ &\to \exp\left\{ N \int dx \left[\exp\left(i \int_0^T dt \vec{\lambda}(t) \cdot \vec{e}(\vec{r}(t)) \right) - 1 \right] \rho(x) \right\} . \end{aligned} \tag{A6}$$

The last equality holds for large N, leading to the identification

$$G[\vec{\lambda}] = N \int dx \left[\exp\left(i \int_0^T dt \vec{\lambda}(t) \cdot \vec{e}(\vec{r}) \right) - 1 \right] \rho(x). \tag{A7}$$

This derivation is sensible only if (A7) becomes independent of N in the limit of large N. For the example considered in the text, the equilibrium state is

$$\rho(x) = V^{-1}(\beta m/2\pi)^{3/2} \exp(-\beta m v^2/2) \equiv V^{-1}\phi(v) \tag{A8}$$

and (A7) becomes

$$G[\vec{\lambda}] = n \int d\vec{r} d\vec{v} \phi(v) \left[\exp\left(i \int_0^T dt \vec{\lambda}(t) \cdot \vec{e}(\vec{r} + \vec{v}t) \right) - 1 \right], \tag{A9}$$

where $n \equiv N/V$ is the number density. Clearly, $G[\vec{\lambda}]$ is intensive for large N, V. In summary, (A9) illustrates that any property of the electric field dynamics can be reduced to quadratures for the simple model considered here. The many-body problem has been treated exactly, as expected for noninteracting particles. The final analysis for a given property still may be complex, but the results are numerically accessible.

The one- and the two-time generating functions considered in Sec. II are obtained from (A9) by the choices $\vec{\lambda}(t) \to \vec{\lambda}\delta(t - t_1)$ and $\vec{\lambda}(t) \to \vec{\lambda}_1\delta(t - t_1) + \vec{\lambda}_2\delta(t - t_2)$, respectively,

$$\begin{aligned} G[\vec{\lambda}] \to G(\vec{\lambda}) &= n \int d\vec{r} d\vec{v} \phi(v) \left\{ \exp[i\vec{\lambda} \cdot \vec{e}(\vec{r} + \vec{v}t_1) - 1] \right\} \\ &= n \int d\vec{r} d\vec{v} \phi(v) \left\{ \exp[i\vec{\lambda} \cdot \vec{e}(\vec{r})] - 1 \right\}, \end{aligned} \tag{A10}$$

$$\begin{aligned} G[\vec{\lambda}] \to G(\vec{\lambda}_1, \vec{\lambda}_2; t_2 - t_1) &= n \int d\vec{r} d\vec{v} \phi(v) \left\{ \exp[i\vec{\lambda}_2 \cdot \vec{e}(\vec{r} + \vec{v}t_2) + i\vec{\lambda}_1 \cdot \vec{e}(\vec{r} + \vec{v}t_1)] - 1 \right\} \\ &= n \int d\vec{r} d\vec{v} \phi(v) \left\{ \exp[i\vec{\lambda}_2 \cdot \vec{e}(\vec{r} + \vec{v}(t_2 - t_1)) + i\vec{\lambda}_1 \cdot \vec{e}(\vec{r})] - 1 \right\}. \end{aligned} \tag{A11}$$

The second equalities of (A10) and (A11) follow from the change of variables $\vec{r} \to \vec{r} + \vec{v}t$ (expressing time translational invariance for the equilibrium state). These are the results used in Sec. II.

APPENDIX B: DETAILED RESULTS

In this appendix the general expressions for the distribution of field values $Q(\vec{\epsilon})$, the distribution of field derivative values $P(\vec{\eta})$, the autocorrelation function $C(t)$, and the conditional electric field $\vec{\mathcal{E}}(t \mid \vec{\epsilon})$ are reduced to simple integral forms suitable for numerical evaluation.

1. Distribution of field values $Q(\vec{\epsilon})$

According Eq. (21) it is sufficient to consider the distribution of field magnitudes, given by $q(\epsilon) = 4\pi\epsilon^2 Q(\vec{\epsilon})$. The corresponding dimensionless distribution is $q^*(\epsilon^*) \equiv e_0 q(\epsilon)$, with $\epsilon^* = \epsilon/e_0$. In the following it will be understood that only the dimensionless quantities are considered and the asterisk will be deleted. The angular integrals of (2) and (13) can be performed directly leading to the result

$$q(\epsilon) = (2\epsilon^2/\pi) \int_0^\infty d\lambda \lambda^2 j_0(\lambda\epsilon) e^{G(\lambda)}, \tag{B1}$$

$$G(\lambda) = 3\lambda^{3/2} \int_0^\infty dx x^2 \left\{ j_0[f(x\alpha\sqrt{\lambda})/x^2] - 1 \right\}, \tag{B2}$$

$$f(x) \equiv (1 + x)e^{-x}, \qquad j_0(x) \equiv \sin(x)/x. \tag{B3}$$

2. Distribution of field derivative values $P(\vec{\eta})$

Again, from spherical symmetry, it is sufficient to consider the distribution of magnitudes of the field derivatives $p(\eta) = 4\pi\eta^2 P(\vec{\eta})$. The corresponding dimensionless quantity is $p^*(\eta^*) \equiv \eta_0 p(\eta)$, with $\eta_0 \equiv e_0/t_0$. The angular integrals of (9) are performed, giving (again dropping the asterisks)

$$p(\eta) = (2\eta^2/\pi) \int_0^\infty d\lambda \lambda^2 j_0(\lambda\eta) e^{J(\lambda)}. \tag{B4}$$

$J(\lambda)$ is calculated from the second equation of (9) and (14),

$$J(\lambda) = \lim_{t\to 0} G\left(\frac{\vec{\lambda}}{t}, -\frac{\vec{\lambda}}{t}; t\right)$$
$$= \lim_{t\to 0}(3/4\pi)\int d\vec{r}d\vec{v}\phi(v)\{\exp\{i\vec{\lambda}\cdot[\vec{e}(\vec{r}+\vec{v}t) - \vec{e}(\vec{r})]/t\} - 1\}$$
$$= (3/4\pi)\int d\vec{r}d\vec{v}\phi(v)\{\exp[i\vec{v}\cdot\vec{y}(\lambda, r) - 1]\}, \quad \text{(B5)}$$

where $\vec{y}(\lambda, r)$ is defined by

$$\vec{y}(\lambda, r) \equiv f(r)r^{-3}\left\{\vec{\lambda} + \hat{r}(\hat{r}\cdot\vec{\lambda})\left[3 + \alpha^2 r^2/(1+\alpha r)\right]\right\}. \quad \text{(B6)}$$

The velocity integral can be performed in (B5) to give the final result (in units $r_0 = e_0 = 1$)

$$J(\lambda) = \int_0^\infty dq \frac{3q^2}{2}\exp\left(-\frac{\lambda^2 A(q)}{4}\right)\left(\frac{4\pi}{\lambda^2 B(q)}\right)^{1/2} \times\left[\mathrm{erf}\left(\frac{\lambda\sqrt{B(q)}}{2}\right) - 1\right], \quad \text{(B7)}$$

where

$$A(q) = q^{-6}e^{-2\alpha q}(1+\alpha q)^2,$$
$$B(q) = q^{-6}e^{-2\alpha q}(3 + 3\alpha q + \alpha^2 q^2)(1 + \alpha q + \alpha^2 q^2). \quad \text{(B8)}$$

In the Coulomb case ($\alpha = 0$) the integration in (B7) is performed analytically to yield (17).

3. Field autocorrelation function $C(t)$

The field autocorrelation function is defined by Eq. (10) and the dimensionless form is $C^*(t^*) = C(t)/e_0^2$, with $t^* \equiv t/t_0$ and $t_0 \equiv r_0/u$. Then, using (14) in this definition leads to

$$C(t) = (3/4\pi)\int d\vec{r}d\vec{v}\phi(v)\vec{e}(\vec{r}+\vec{v}t)\cdot\vec{e}(\vec{r}). \quad \text{(B9)}$$

To evaluate the integral, express the single-particle fields in a Fourier representation

$$\vec{e}(\vec{r}) = (2\pi)^{-3}\int d\vec{k}e^{-i\vec{k}\cdot\vec{r}}4\pi\hat{\vec{k}}(k^2+\alpha^2)^{-1}. \quad \text{(B10)}$$

This allows the velocity and the angular coordinate integrals to be performed, with the result

$$C(t) = (12/\pi t)\int_0^\infty dx x^4(x^2 + \alpha^2 t^2/4)^{-2}e^{-x^2}. \quad \text{(B11)}$$

It may be verified that this is equivalent to the result in Ref. [5] (using an integration by parts),

$$C(t) = (6/\sqrt{\pi}t)F(\alpha t/2),$$
$$F(x) \equiv 1 + x^2 - \sqrt{\pi}(\tfrac{3}{2} + x^2)xe^{x^2}\mathrm{erfc}(x). \quad \text{(B12)}$$

Here $\mathrm{erfc}(x)$ denotes the complementary error function.

4. Conditional electric field $\vec{\mathcal{E}}(t \mid \vec{\epsilon})$

From (24), (12), and (14) the dimensionless scalar function determining $\vec{\mathcal{E}}(t\,|\,\vec{\epsilon})$ is given by

$$C(t\,|\,\epsilon) = \vec{\epsilon}\cdot\langle\vec{E}(t)\delta(\vec{\epsilon} - \vec{E})\rangle/Q(\vec{\epsilon})\epsilon^2$$
$$= [3/q(\epsilon)](2\pi)^{-3}\int d\vec{\lambda}e^{-i\vec{\lambda}\cdot\vec{\epsilon}+G(\lambda)}\int d\vec{r}d\vec{v}\phi(v)\vec{\epsilon}\cdot\vec{e}(\vec{r})e^{i\vec{\lambda}\cdot\vec{e}(\vec{r}+\vec{v}t)}$$
$$= [3/q(\epsilon)](2\pi)^{-3}\int d\vec{\lambda}e^{G(\lambda)}\int d\vec{r}d\vec{v}\phi(v)\vec{\epsilon}\cdot\vec{e}(\vec{r}-\vec{v}t)e^{i\vec{\lambda}\cdot[\vec{e}(\vec{r})-\vec{\epsilon}]}. \quad \text{(B13)}$$

The field $\vec{e}(\vec{r}-\vec{v}t)$ can be given a Fourier representation and all angle integrals performed by spherical harmonics expansions. The resulting final expression is

$$C(t\,|\,\epsilon) = 3[4\pi^3 Q(\epsilon)]^{-1}\int_0^\infty d\lambda\lambda^{5/2}e^{G(\lambda)}j_1(\lambda\epsilon)\varphi(\lambda), \quad \text{(B14)}$$

where

$$\varphi(\lambda) = \int_0^\infty d\xi\xi^{-2}\Omega((\lambda/\xi)^{1/2}, t)j_1[\xi f(\alpha(\lambda/\xi)^{1/2})],$$
$$\Omega(r,t) = f(\alpha r)\int_{-r/t}^\infty dx e^{-\alpha t x - x^2} + f(-\alpha r)\int_{r/t}^\infty dx e^{-\alpha t x - x^2} - (2/t)e^{-(r/t)^2}, \quad \text{(B15)}$$

where $f(x)$ is defined in (B3) and $j_1(x) = x^{-2}[\sin(x) - x\cos(x)]$ is the spherical Bessel function of order 1.

APPENDIX C: SINGLE-PARTICLE FIELDS

In this appendix dynamics of fields due to a single particle are considered. In the limit of large fields and short times the corresponding properties agree with those of Appendix B for the total field [8]. Otherwise, these single-particle field properties only provide some qualitative guidance for interpreting the results of Appendix B.

The calculations are straightforward, so only the results are quoted. For the distribution of field values $Q_1(\vec{\epsilon})$,

$$q_1(\epsilon) = 4\pi\epsilon^2 Q_1(\vec{\epsilon}) \equiv 4\pi\epsilon^2 N\langle\delta(\vec{\epsilon} - \vec{e}(\vec{r}_1))\rangle = 3R^2(\epsilon)\{\,|\,\tfrac{d}{dr}[f(r)/r^2]\,|_{r=R(\epsilon)}\}^{-1}, \tag{C1}$$

where $R(\epsilon)$ is the solution to $\epsilon = f(R)/R^2$. For distribution of field derivative values $P_1(\vec{\epsilon})$,

$$p_1(\eta) = 4\pi\eta^2 P_1(\eta) \equiv 4\pi\eta^2 N\langle\delta(\vec{\eta} - \vec{e}\,(\vec{r}_1))\rangle = 6\pi^{3/2}\eta^2 \int_0^\infty dR\phi\left(\frac{\eta}{A(R)}\right)\frac{R^2}{A^2(R)[A(R)+B(R)]\sqrt{Z(R)}}\mathrm{erf}\left]\sqrt{Z(R)}\right], \tag{C2}$$

where

$$Z(R) = \frac{B(R)\eta^2[2A(R)+B(R)]}{A^2(R)[A(R)+B(R)]^2},$$

$$A(R) = f(R)/R^3, \qquad B(R) = R\left[f(R)/R^3\right]'_R.$$

For the field autocorrelation function $C_1(t)$,

$$C_1(t) \equiv N\langle\vec{e}(\vec{r}_1(t))\cdot\vec{e}(\vec{r}_1)\rangle. \tag{C3}$$

This is the same as (B9), so $C_1(t) = C(t)$ given by (B11) or (B12). For the conditional electric field $\vec{\mathcal{E}}_1(t\mid\vec{\epsilon})$,

$$\vec{\mathcal{E}}_1(t\mid\vec{\epsilon}) \equiv N\langle\vec{e}(r(t))\delta(\vec{\epsilon}-\vec{e})\rangle/Q(\vec{\epsilon}) = C_1(t\mid\epsilon)\vec{\epsilon}, \tag{C4}$$

$$C_1(t\mid\epsilon) = N\vec{\epsilon}\cdot\langle\vec{e}(r(t))\delta(\vec{\epsilon}-\vec{e})\rangle/Q(\vec{\epsilon})\epsilon^2, \tag{C5}$$

$$C_1(t\mid\epsilon) = (4\pi/\alpha t)\int_0^{R/t} dv v\phi(v)\sinh(\alpha t v) + (4\pi/\alpha t\epsilon R^2)[\sinh(\alpha R) - \alpha R\cosh(\alpha R)] \times \int_{R/t}^\infty dv v\phi(v)e^{-\alpha v t}. \tag{C6}$$

APPENDIX D: EVALUATION OF THE KANGAROO EXPONENT

The exponent $\nu(\epsilon)$ for the kangaroo process is defined by Eq. (30). To determine $\nu[\epsilon)$ from this equation it is convenient to perform the angular integrals and change the integration variable ϵ to $\nu(\epsilon)$,

$$C(t) = \int_0^\infty d\nu[\tfrac{d\epsilon}{d\nu}4\pi\epsilon^4 Q(\epsilon)]e^{-\nu t}. \tag{D1}$$

With the assumed boundary conditions $\nu(0) = 0$ and $\nu(\infty) = \infty$. This shows that $C(t)$ is the Laplace transform of the function of ν defined by the square brackets on the right-hand side of (D1). The Laplace transform can be inverted to obtain an equation that determines $\nu(\epsilon)$ in terms of the inverse transform of $C(t)$ [2,7],

$$\frac{d\epsilon}{d\nu}4\pi\epsilon^4 Q(\epsilon) = \int_{-\infty+i\eta}^{\infty+i\eta}\frac{dt}{2\pi i}e^{\nu t}C(t). \tag{D2}$$

Integrating this equation gives

$$\int_0^\epsilon d\epsilon_1 4\pi\epsilon_1^4 Q(\epsilon_1) = \int_{-\infty+i\eta}^{\infty+i\eta}\frac{dt}{2\pi i}t^{-1}\,(\,e^{\nu t}-1\,)\,C(t). \tag{D3}$$

The right-hand side is now evaluated using the explicit form (B12) for $C(t)$. This is facilitated by using the identity

$$\int_0^\infty e^{-st}e^{-t^2}dt = \frac{\sqrt{\pi}}{2}e^{s^2/4}\mathrm{erfc}(s/2). \tag{D4}$$

After some algebra we find

$$\int_0^\epsilon d\epsilon_1 4\pi\epsilon_1^4 Q(\epsilon_1) = \frac{6\nu(\epsilon)}{\pi} - \frac{3\alpha}{2}\mathrm{erf}\left(\frac{\nu(\epsilon)}{\alpha}\right) + \frac{3\nu(\epsilon)}{\sqrt{\pi}}\exp\left(-\frac{\nu^2(\epsilon)}{\alpha^2}\right). \tag{D5}$$

Since $Q(\epsilon)$ is known, the left-hand side can be calculated as a function of ϵ and the right-hand side inverted to find $\nu(\epsilon)$.

[1] R. Stamm, B. Talin, E. Pollock, and C. Iglesias, Phys. Rev. A **34**, 4144 (1986).

[2] A. Brissaud and U. Frisch, J. Quant. Spectrosc. Radiat. Transfer **11**, 1767 (1971); J. Seidel, Z. Naturforsch. Teil A **32**, 1195 (1977); in *Spectral Line Shapes*, edited by B. Wende (de Gruyter, New York, 1981); J. Dufty, *ibid.*

[3] J. Holtsmark, Ann. Phys. (Leipzig) **58**, 577 (1919).

[4] S. Chandrasekhar, Revs. Mod. Phys. **15**, 1 (1943).

[5] M. Rosenbluth and N. Rostoker, Phys. Fluids **5**, 776 (1962).
[6] R. Stamm and E. Smith, Phys. Rev. A **30**, 450 (1984); E. Smith, R. Stamm, and J. Cooper, *ibid.* **30**, 454 (1984).
[7] N. van Kampen, *Stochastic Processes in Physics and Chemistry* (North-Holland, Amsterdam, 1981); A. Brissaud and U. Frisch, J. Math. Phys. **15**, 524 (1974).
[8] J. W. Dufty and L. Zogaib, in *Strongly Coupled Plasma Physics*, edited by S. Ichimaru (Elsevier Science, Amsterdam, 1990); J. W. Dufty and L. Zogaib, Phys. Rev. A **44**, 2612 (1991).
[9] A. Alastuey, J. Lebowitz, and D. Levesque, Phys. Rev. A **43**, 2673 (1991).
[10] C. A. Iglesias, J. L. Lebowitz, and D. MacGowan, Phys. Rev. A **28**, 1667 (1983); J. W. Dufty, in *Strongly Coupled Plasma Physics*, edited by F. J. Rogers and H. E. DeWitt (Plenum, New York, 1987).
[11] J. W. Dufty and L. Zogaib, Phys. Rev. A **47**, 2958 (1993).
[12] J. P. Hansen and I. R. McDonald, *Theory of Simple Fluids* (Academic, New York, 1986).